Available online at www.sciencedirect.com

ScienceDirect

Journal of Magnesium and Alloys 12 (2024) 490–505

www.elsevier.com/locate/jma

Review

Photocatalytic application of magnesium spinel ferrite in wastewater remediation: A review

Rohit Jasrotia[a,b,c,1,*], Nikhil Jaswal[a,1], Jyoti Prakash[a], Chan Choon Kit[c], Jagpreet Singh[d], Abhishek Kandwal[a,c,e,*]

[a] School of Physics and Materials Science, Shoolini University, Bajhol, Solan, H.P., India
[b] Himalayan Centre of Excellence in Nanotechnology, Shoolini University, Bajhol, H.P., India
[c] INTI International University, Putra Nilai, Negeri Sembilan, Malaysia
[d] Department of Chemistry, University Centre for Research & Development Chandigarh University, Mohali, 140413, Punjab, India
[e] Shenzhen Institute of Advanced Technology, Chinese Academy of Sciences, China

Received 20 October 2023; received in revised form 2 February 2024; accepted 5 February 2024
Available online 28 February 2024

Abstract

This review paper explores the efficacy of magnesium ferrite-based catalysts in photocatalytic degradation of organic contaminates (antibiotic and dyes). We report the influence of different doping strategies, synthesis methods, and composite materials on the degradation efficiency of these pollutants. Our analysis reveals the versatile and promising nature of magnesium ferrite-based catalysts, offering the valuable insights into their practical application for restoring the environment. Due to the smaller band gap and magnetic nature of magnesium ferrite, it holds the benefit of utilising the broader spectrum of light while also being recoverable. The in-depth analysis of magnesium ferrites' photocatalytic mechanism could lead to the development of cheap and reliable photocatalyst for the wastewater treatment. This concise review offers a thorough summary of the key advancements in this field, highlighting the pivotal role of the magnesium ferrite based photocatalysts in addressing the pressing global issue of organic pollutants in wastewater.

Keywords: Magnesium ferrite; Wastewater; Dyes; Antibiotics; Photocatalytic degradation.

1. Introduction

The textile sector is well-known for high effluent generation and environmental contamination [1]. This sector is considered as one of the main significant pollutant producer for the ground and surface water reservoirs due to its extensive usage of water and usage of over 8000 chemicals [2]. Textile businesses normally produce 200–350 m^3 of the wastewater, producing 100 kg of chemical oxygen demand per tonne of end product [3,4]. The effluent from the industries contains both organic and inorganic pollutants. Amidst numerous organic-contaminates, the most prominent ones are dyes and antibiotics which are very harmful and complex due to their structure. There are various types of synthetic dyes which are currently being used ranging from azo dyes, disperse dyes, vat dye, reactive dye, sulphur dye etc. [5]. The aquatic life is being impacted in a grave manner due to these dyes. The dyes lowers the dissolve oxygen value in the water bodies by blocking the sunlight [6]. It also have very adverse effects on the human health, [7] such as azo dyes components can cause the human bladder cancer, and other biological problems such as eye and skin irritation [8,9]. Antibiotics are the other organic compounds that cause harm to the nature, and also, their excess presence in the environment is an alarming situation for the humans. Many research studies shows that there are different antibiotics present in the water such

* Corresponding authors.
E-mail addresses: rohitsinghjasrotia4444@gmail.com (R. Jasrotia), abhishekandwal@gmail.com (A. Kandwal).
[1] Rohit Jasrotia and Nikhil Jaswal have contributed equally as co first authors.

https://doi.org/10.1016/j.jma.2024.02.006

as sulfamethoxazole, ciprofloxacin and tetracycline [10,11]. Excess presence of antibiotics in the surroundings can cause the growth of antibiotic resistive bacteria in the water bodies which could be harmful for not only the current generation but also for the future generation [12].

To counter these emerging organic pollutants, different methods of water purification has been developed some of which are a) adsorption b) catalytic process c) membrane process d) ionising radiation process, and e) magnetically assisted process, etc. These methods are used for the purification of water but most of these methods are not much effective in degrading the organic compounds [13]. One approach which is still maturing and shows potential for the organic waste treatment is the photocatalysis [14,15]. This process is consider effective and green method [16] as it utilises the sunlight and also shows higher degradation efficiencies [17]. This process requires catalysts to carry out the degradation. Among different materials, semiconductor is considered as the most effective materials to be used as photocatalysts. They can be easily removed from the system and are produced cheaply [18]. Some of the widely utilized photocatalysts are TiO_2 and ZnO, and both of these materials shows strong oxidation tendencies but their large band gap and low visible light utilisation limit their usage at large scale. To tackle these limitations, researchers have shifted their interest from these materials to spinel ferrites due to their lower band gap and inexpensive nature. The formula for spinel ferrite is AB_2O_4 [19,20], here A and B represents divalent and trivalent metallic cations, [14] and they are frequently employed as the magnetic photocatalysts [21]. Among the numerous types of ferrites, there are only few spinel ferrites that show relatively the more potential to be used as a photocatalyst. One such material is magnesium ferrite. Magnesium ferrite is a spinel magnetic oxide with a chemical formula of $MgFe_2O_4$. Mg ferrite is widely utilised in various magnetic applications while also being used as catalyst [22]. Magnesium ferrite is n-type semiconducting material, and is a soft magnet with small band gap range [23]. Magnesium ferrite is being considered as good catalyst than the other catalysts because of its excellent chemical and thermal stability, making it more adaptive for the hard environment conditions [24]. The saturation magnetisation of the magnesium ferrite is high which facilitate the separation of catalyst from the water by applying the magnetic field [24]. It has a high capacity for the charge migration as well as charge separation efficiency, making it more reactive and less susceptible to recombination [25]. Fig. 1 illustrates the importance of magnesium ferrite as a photocatalyst.

There are various methods for the production of magnesium ferrite such as microwave sintering, co-precipitation and sol-gel which can affect its size, shape and defect structure. This impact ultimately affect its photocatalytic efficiencies [26].

In this review paper, we will discuss about the conventionally used synthesis approaches and their limitations when dealing with the organic pollutants. We will also go over the several dyes and antibiotics that are being used on a large scale in industry and are harmful for the environment and human well-being. This investigation will demonstrate the significance of photocatalysis in the removal of organic contaminants and the advantages of using magnesium ferrite as a photocatalyst. We will also discuss the impact of various factors like synthesis, dopants, and elementary compositions on the efficiency of photocatalysis. This study will also cover the properties of magnesium ferrite which can affect the efficiency of the photocatalysis i.e., structural, magnetic, and optical.

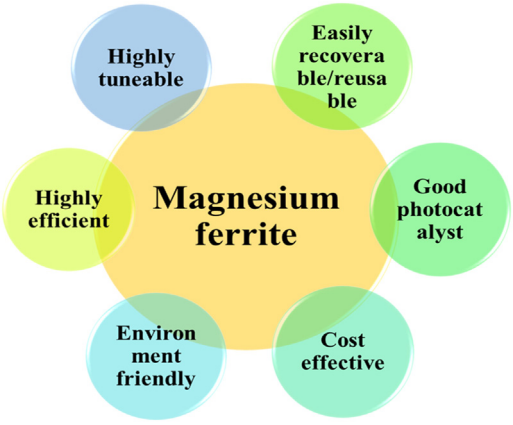

Fig. 1. Magnesium ferrite as a photocatalyst.

2. Wastewater causes and remedies

One of the most difficult problems the world is currently confronting is water pollution. The harmful contaminants in rivers and other water resources are affecting the environment very badly. On the basis of waste water production, the waste water is mainly classified into four categories which are industrial, domestic, infiltration/inflow and storm water [27]. Industrial pollution is caused via the release of toxic and harmful chemicals from the factories into the water resources. These chemicals are present in various forms such as solid, liquid and gaseous [28]. The various pollutants from these different resources are mainly classified into two types, inorganic and organic pollutants. The former mainly include cations, heavy metals, radioactive debris, halides and oxyanion materials [29] and the later includes dyes [30] and antibiotics [31]. According to a 2017 UN Water UNESCO research, high-income nations treat about the 70% of municipal and industrial wastewater, as compared to the 38% of the upper-middle-income countries, 28% of lower-middle-income countries, and 18% of low-income countries. Given current trends, it is expected that nearly 80% of global wastewater is being released without treatment [32]. Although there are conventional approaches being used for the treatment of water but these methods possess limitations, including the need for the addition of reusable chemicals, specific pH requirements for the effluents, and the low biodegradability of certain molecules (such as dyes). To address these challenges, a novel and emerging solution is the advanced oxidation processes (AOPs) [33–35]. The AOP consist of set of treatments

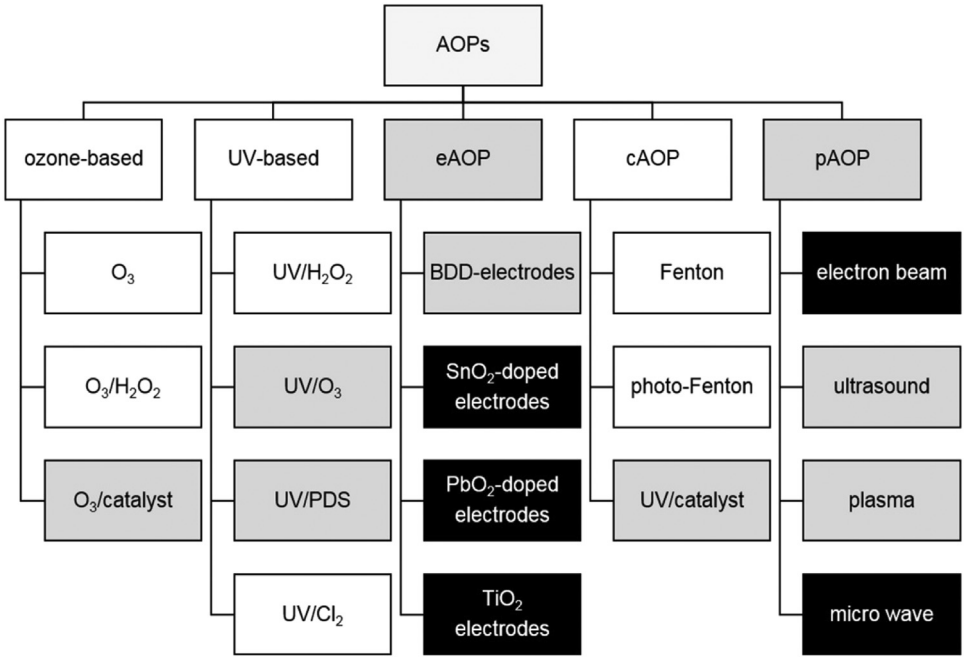

Fig. 2. Schematic representation of different AOPs, representing large scale(white), pilot scale(grey) and lab scale (black) (reprinted with permission from [36]).

that treats the waste water using the strong oxidising agents. Advance oxidation is further classified into five parts which are electrochemical oxidation process, ultraviolet (UV) based, ozone based, catalytic AOP, physical AOP and Photocatalytic AOPs as mentioned in Fig. 2 [36].

Among the various AOPs, the photochemical AOPs are considered the most efficient one for elimination of organic pollutants as they can reduce the contaminants to the less harmful compounds by using the strong oxidising agents produced during the reaction. These radicals can decompose most of the stable organic contaminates which are a lot harder to degrade via the conventional approaches [37]. Also, the photocatalysis doesn't cause any secondary waste and it can entirely oxidises the contaminants to innocuous compounds such as water and carbon dioxide [38]. It is useful method as it uses the solar energy for starting the reaction which is eco-friendly, reusable and ample in nature [39,40]. A detailed explanation on the photocatalytic process is given in the section ahead.

3. Photocatalytic degradation

A photoinduced reaction that is catalysed, or made faster by the presence of light, is known as photocatalysis. This process can be carried out directly by irradiating the reaction or indirectly by irradiating the catalysts. The purpose of this irradiation is to lower the activation energy to carry out the reaction. It could either happens naturally or synthetically by using the catalysts. The natural photocatalysis occurs in the presence of chlorophyll during the photosynthesis. Whereas, the catalyst based photocatalysis was first discovered by Honda and Fujishima in 1972 via the TiO_2 electrode under the UV irradiation [41]. In catalyst based photocatalysis, the redox reaction occurs due to formation of strong reducing agents like the hydroxyl radicals.

The photocatalysis is largely influenced by the type and traits of the catalyst. During this process, the catalyst absorbs the photons which causes the excitation of the electrons from the valence to the conduction band. The produced exitons (holes and electrons) helps to carryout the photocatalysis. The first basic condition for the photocatalysis is that the energy of photons falling onto the catalysts should be equal or more than the band gap of the catalyst. There are three conditions that are required to be present in an ideal photocatalysts, which are i) ability to harvest the broad spectrum of light, ii) separation of exitons from the bulk to the surface of catalysts and iii) the contribution of interfacial charges in the redox reactions at the reactive sites [42,43]. These three conditions depends on the various factors like band gap, crystallite size, surface area, porosity, etc. [44]. The lower size could cause the quantum confinement by making the band gap energies more distinct and thus, increasing the light utilisation. Also, the smaller band gaps leads to the improved light absorption over a wide spectrum. But there is also a chance of increasing the recombination rate of exitons produced which can be reduced by making use of electron trapping reagents like H_2O_2. Further more, the catalysts used during photocatalysis can be divided into two major categories, i.e., homogeneous and heterogeneous catalysts. The homogeneous catalysts are in aqueous phase and thus, are more effective in degrading the pollutants, but the separation of homogeneous catalyst is a difficult task. On contrary, the heterogeneous catalysts are in solid phase hence can be easily separated out of the solution after the reaction. Generally, the heterogeneous pho-

tocatalysis is considered to be the more viable option because it leaves the possibility of reusing the photocatalysts and thus, increasing the efficiency and inexpensiveness of the photocatalysis.

The heterogeneous catalysis utilises the solid semiconducting catalysts due to their appropriate optical traits. There are different kind of semiconductors including binary (ZnO, TiO_2, CdS, g-C_3N_4, etc.), ternary (Perovskite, spinels, etc.) and quaternary semiconductors (AlGaInP, Cu_2ZnSnS_4, etc.) that can be utilised for the purpose of photocatalysis [45,46]. Out of these three types, the ternary semiconductors are mostly utilised as the heterogeneous catalysts due to their higher stability and higher number of active sites which can promote the various reaction during the process of photocatalysis. The researchers are continuously trying to optimise the band gap and charge separation of the semiconductors in order to increase their efficiency as photocatalysts [47].

The photocatalysis mechanism is mainly divided into two parts-direct mechanism and indirect mechanism. In direct method, the pollutant can absorb the photon energy and achieve an excited state which in-turn get converted to the semi-oxide cation. This cation species can trap the conduction band's electrons from the photocatalyst and cause the formation of superoxide radical by using the dissolved oxygen. Similar reaction can occur over the valence band and can cause the formation of hydroxyl radicals. These radicals are helpful in degrading the organic pollutants, and also, this type of method is generally followed by dye molecules. In case of indirect catalysis, the pollutants doesn't get excited and the reaction is carried out by photo-induced electrons of the photocatalyst. The electron of photocatalyst engage with the photons and hops to the conduction band, where it can react with the adsorbed oxygen species on the photocatalysis and cause the formation of superoxide radicals. The holes also ionises the water and causes the formation of hydroxyl radical. These reactive species can then react with the organic pollutants and degrade them to other less harmful products like CO_2 and H_2O [48]. Furthermore, the types of pollutants being degraded also impact the photocatalysis process. The movement of electron and holes are different for unlike pollutants during the photocatalytic degradation for e.g., in dyes, the dye molecules serve as both electron donors and acceptors. The water molecules over the catalyst surface oxidises when they come into contact with the holes during the photocatalysis, creating hydroxyl radicals. Additionally, superoxide or hydroperoxyl radicals form when the oxygen molecules present in the solution gets reduced via the electrons. Then, it leads to the production of other reactive oxygen species (ROS) like superoxide (O^{2-}) and hydroxyl radical (OH^-), helping in oxidation of pollutant. These ROS then proceed to attack and breakdown the contaminants. The ROS are the primary species responsible for the pollutant degradation [49–51]. Fig. 3 gives the mechanism of this approach. There are some factors that affects the degradation efficiency of pollutants including a) pollutant concentration b) quantity of catalyst c) reaction medium of pH d) type and configuration of the catalyst e) light intensity.

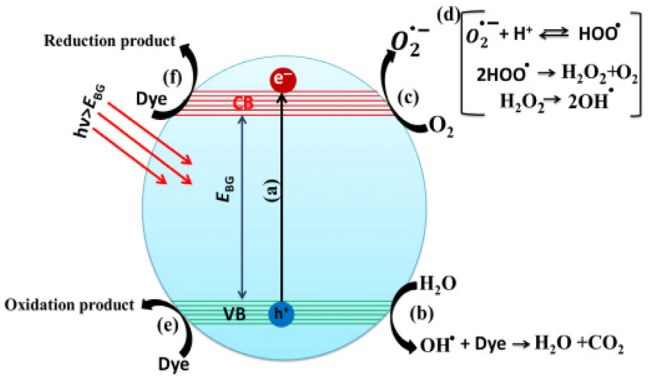

Fig. 3. Schematic representation of photocatalytic degradation (reprinted with permission from [48]).

a) Pollutant concentration: The initial amount of pollutants influence the adsorption equilibrium and the presence of active sites on the photocatalyst surface. Low beginning concentrations can promote the pollutant adsorption and degradation, whereas the high initial concentrations can lead to active site saturation and competition. Additionally, a high initial concentration may inhibit light penetration and diminish the photocatalytic effectiveness [39].
b) Amount of catalyst: The photocatalytic system's surface area and light absorption are influenced by the catalyst's quantity. Increasing the catalyst concentration can boost the photodegradation rate by growing the number of active sites. Beyond a certain threshold, however, the additional catalyst may not continue to increase the efficiency but rather result in the aggregation and shading effects that lower the light utilisation [39].
c) Reaction medium pH: The pH of the mixture impacts how the photocatalyst and the pollutant adsorb and charged their surfaces. Depending on the kind of photocatalyst and the pollutant used in the reaction, the ideal pH will vary. In general, an acidic pH can encourage the production of hydroxyl radicals and enhance the oxidation potential of system. However, some photocatalysts may corrode and dissolve in the presence of an excessively low pH [39].
d) Type and composition of catalyst: different photocatalysts have unique characteristics that affect how well they can produce ROS and breakdown pollutants, including band gap, surface area, crystallinity, and stability. As an illustration, due to its great stability, low cost, and strong oxidising power, TiO_2 is a well-liked photocatalyst. Nevertheless, TiO_2's efficiency is constrained as it only absorb the ultraviolet light. To increase TiO_2's visible light activity, the different changes including doping, coupling, and sensitising have been applied [50].
e) Light Intensity: The quantity of photons that arrive at the photocatalyst surface and to start the photodegradation reaction depends on the light intensity. A higher light output can boost the photocatalytic efficiency and

speed up the formation of electron-hole pairs. But, the excessive light output can also have heating effects and also, hasten the recombination of electron-hole pairs [52].

4. Types of organic pollutants

Two types of organic pollutants that causes most of the water pollution are dyes and antibiotics. In this section, we are going to discuss the different type of dyes and antibiotics in detail.

4.1. Dyes

Dyeing is the process of colouring materials including fabrics, paper, leather, and other items with chemical compounds, and they are mainly of two types-natural and synthetic. In the past, dyes were made from the natural materials, however, William Henry Perkin committed an unintended error in 1856 and made the first synthetic dye to be commercially successful. After that by the end of nineteenth century, over thousands of synthetic dyes have been manufactured [53]. These dyes are commonly categorised as: cationic dyes, non-ionic dyes and anionic dyes. In an aqueous solution, cationic dyes, commonly referred to as basic dyes can be separate into positively charged ions [54]. Some of the examples of cationic dyes are crystal violet (CV) and methylene blue (MB) [55]. Anionic dyes are a particular class of colour that, when dissolved in water, take on a negative charge. They are used to colour textiles like nylon, silk, and wool because they are usually water soluble [56]. Some of the examples of anionic dyes are Congo red, Cochineal Red A and Acid Red 14 [57]. Non-ionic dyes are a particular kind of dye that, when dissolved in the water, have no electrical charge. They are used to colour fabrics like polyester, acetate, and nylon and are normally water-insoluble or only marginally soluble. Because they are applied by dispersing them in a carrier solution that aids in their penetration of the fibres, non-ionic dyes are also known as disperse dyes [56]. Dyes like malachite green (MG) are an example of non-ionic dyes [58]. The most common form of dyes is cationic, while the anionic dyes are acidic dyes and contain a variety of dyes such as azo, acid, direct, and reactive dyes. Some of the most used dyes are discussed below.

4.1.1. Rhodamine B (RhB)

RhB is a cationic dye and come under the Xanthene class of basic dye [59]. These synthetic dyes are the earliest kind of dyes and are employed in a variety of applications. These are water soluble and are used in animal treatments, biological trial staining, printing, and the textile sector. RhB's IUPAC designation is N-[9-(ortho-carboxyphenyl)-6-(diethylamino)-3H-xanthen-3-yli-dene] diethyl ammonium chloride, and Fig. 4 shows its chemical structure. Its molecular weight is 479.02 g mol^{-1} and a maximum wavelength absorbance (A) is 554 nm [60]. RhB is difficult to remove using the standard techniques because it is resistant to biodegradation and contains a lot of salts [61,62]. The side effects of rhodamine B include tissue necrosis, elevated heart rate, shock, and vomiting [63]. It can cause the cellular apoptosis and impede the ATP synthase [64]. Therefore, RhB must be eliminated for the protection of environment and the health of living things.

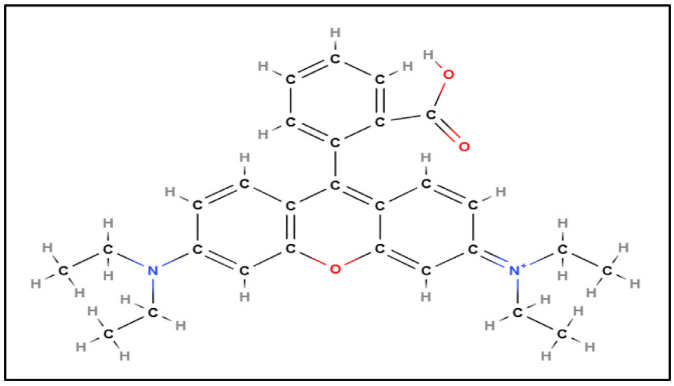

Fig. 4. Structure of Rhodamine B.

4.1.2. Congo red (CR)

In 1883, Paul Bottiger made the discovery of CR dye while working to develop a method for detecting the pH levels. In the cellulose industry, which includes the cotton textiles and paper/pulp, CR dye is often employed because of its high affinity for the cellulose fibres [65]. It is a type of azo dye which is stable against the photo- and biodegradation. Because it has aromatic amines in its structure, it is known to be carcinogenic. Azo dyes are resistant to natural deterioration because they include the aromatic groups [66]. Congo red is known by the IUPAC name, disodium 4-amino-3-[4-[4-[4-(1-amino-4-sulfonato-naphthalen-2-yl) "diazenylphenyl" "phenyl" diazenyl-naphthalene-1-sulfonate. The formula of CR dye is $C_{32}H_{22}N_6Na_2O_6S_2$ and it has a molecular weight and CAS number of 696.66 and 573-58-0. It has maximum wavelength absorbance of 497 nm [67]. CR's organisational structure is illustrated in Fig. 5. Congo red dye has various effects on the health such as it causes skin infection, irritation, cyanosis, vomiting, tissue necrosis and cancer [68,69].

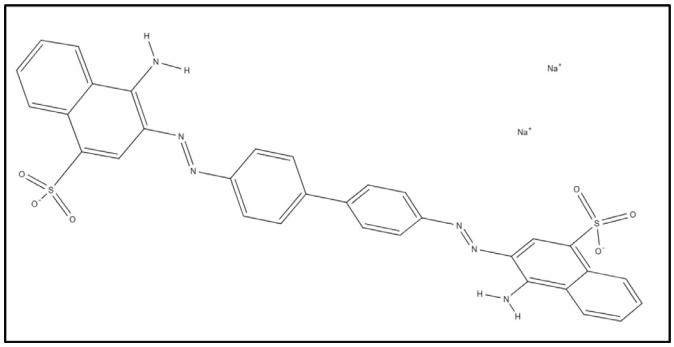

Fig. 5. Structure of Congo red.

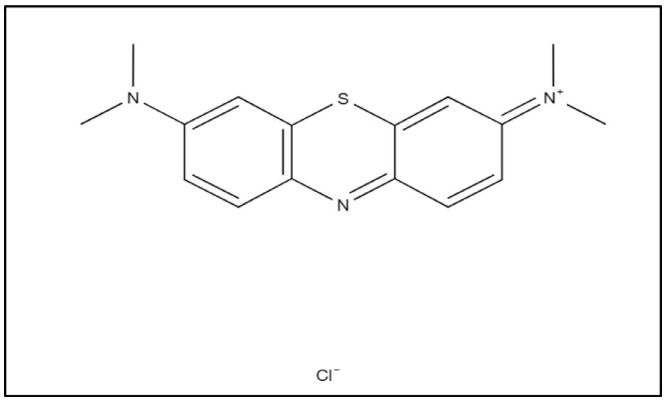

Fig. 6. Illustration of methylene blue structure.

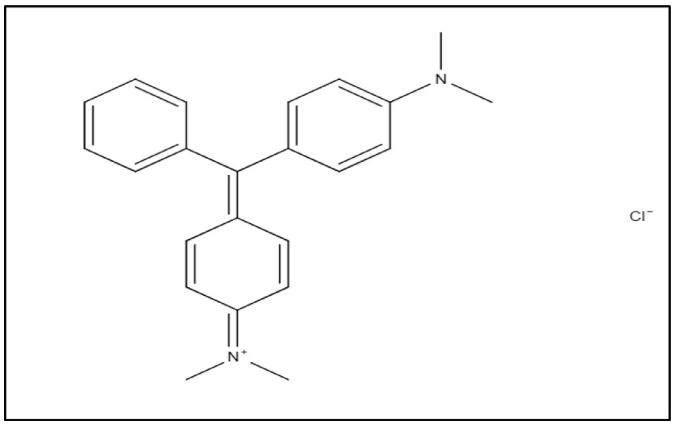

Fig. 7. Structure of Malachite green.

4.1.3. Methylene blue (MB)

MB is a cancer causing toxin which is renowned for its side effects on the aquatic life [70,71]. MB is a type of heterocyclic aromatic complex with a value of 319.85 g/mol molecular weight and $C_{16}H_{18}N_3SCl$ molecular formula. MB is a basic and synthetic type of dye [72] with IUPAC name [3,9-bis dimethyl-aminophenazo thionium chloride]. The maximum wavelength absorbance (A) for the MB is 661 nm [73]. MB is used in the clinical medicine as a antibacterial chemical, colourant and indicator [74]. Heinrich Caro and Soda Fabrik were the first to synthesised the MB in 1876 as a synthetic dye derived from the aniline, which was employed for the purpose of staining cotton [75]. The MB structure is given in Fig. 6.

4.1.4. Malachite green (MG)

MG is a crystalline solid having dark green colour that is made by mixing the strong sulphuric acid or zinc chloride while condensing one part benzaldehyde with two parts diemethylaniline. MG is a triarylmethane dye ($C_{23}H_{26}N_2O$, Cl 42,000) [76]. It is referred by IUPAC nomenclature, [4-[[4-(dimethylamino)phenyl].-phenylmethylidene]cyclohexa-2,5–dien-1-ylidene]chloride, -dimethylazanium, with a molecular weight and a maximum wavelength absorbance (A) of 364.911 g/mol and 619 nm [77].

Fig. 7 illustrates the structure of MG. MG is a biocide that is broadly utilised in the fish farming sector universally. It is quite good at preventing the serious protozoal and the fungi infections [78,79]. Additionally, MG is employed in the wool, paper, cotton, and acrylic trades as both dye and medical decontaminator, and anthelminthic [80]. MG has a great impact on the reproductive system, and immunity with cancer and genotoxic causing traits [81,82].

4.2. Antibiotics

The most effective class of medications ever created for enhancing the human health is undoubtedly the antibiotics. Apart from this essential function, antibiotics (generally speaking, antimicrobials) have also been utilised for treating and preventing the diseases in plants and animals, fostering growth in animal farming, and many more [83]. Antibiotics inhibit or prevent the micro-organisms growth. Antibiotics are categorised into numerous types depending on their structure, mechanism, and the mode of administrations [84]. The antibiotics have mainly divided into five different class like β-Lactams, Fluoroquinolones, Macrolides, Sulfonamides, Tetracyclines with few more classes of antibiotics such as Chloramphenicol, Lincomycin and Trimethoprim [12]. WHO stated that the presence of antibiotics in environment for a long time can make the bacteria resistant to the antibiotics and there will be no effect of antibiotics to the bacteria as there is a development of antibiotic-resistant genes [85].

Here we have discussed the antibiotics like tetracycline and ciprofloxacin, since these are commonly used antibiotics that pose a risk to the ecosystem and general people due to their solubility, persistence, toxicity, and probable carcinogenicity [86].

4.2.1. Ciprofloxacin

Ciprofloxacin are the most famous antibiotics of 1990s with the sales greater than 1 billion in hospitals. These antibiotics have a chemical formula $C_{17}H_{18}FN_3O_3$ [87]. IUPAC designation for the ciprofloxacin is 1-cyclopropyl-6-fluoro-4-oxo-7-piperazin-1-ylquinoline-3-carboxylic acid and also has a molar mass 331.34 $g.mol^{-1}$ [88]. Ciprofloxacin is mostly prescribed to treat the lung disorders, skin infections, STIs, and urinary tract infections [89]. Different surveys from the hospital has shown the presence ciprofloxacin within the waste water like Seifrtová et al. has found that the concentration of ciprofloxacin is 150 μg/L in hospital waste waster [90]. In another study by Larsson et al., it was found that the concentration of ciprofloxacin in pharmaceutical waste water lies between 31 and 50 mg/L [91]. In one of the research conducted for ciprofloxacin presence in drinking water, the presence of ciprofloxacin was found to be 6.5 μg/l [92]. The presence of ciprofloxacin in the environment is effecting the microalga such as *Pseudokirchneriella subcapitata* and *Lemna minor* growth [93]. The structure of ciprofloxacin is mentioned in Fig. 8.

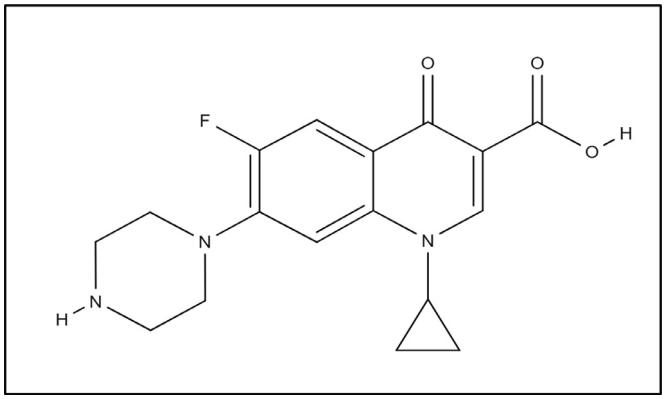

Fig. 8. Chemical structure of ciprofloxacin.

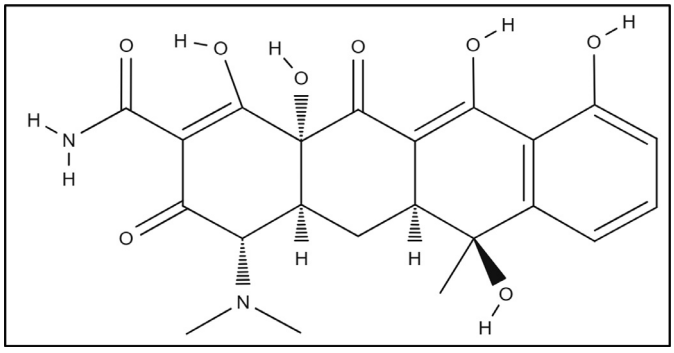

Fig. 9. Chemical structure of Tetracycline.

4.2.2. Tetracycline

Tetracycline is a type of antibiotic that is used for the treatment of acne, cholera and malaria in animals and humans [94]. Tetracycline have a chemical formula and a molar mass of $C_{22}H_{24}N_2O_8$ and 444.44 $gmol^{-1}$. IUPAC name for the tetracycline is (4S,4aS,5aS,6S,12aR)-4-(dimethylamino)−1,6,10,11,12a-pentahydroxy-6-methyl-3,12-dioxo-4,4a,5,5a tetrahydrotetracene-2-carboxamide. Antibiotics like like tetracycline are chemically stable and highly soluble in water which make it hard to degrade by the conventional methods [95]. Tetracycline has a track record of past three generations. First generation of tetracyclines contain all the natural antibiotics such as tetracycline oxytetracycline and chlortetracycline. Second generation of tetracyclines contain antibiotics like doxycycline and minocycline. The third generation tetracylines contain antibiotic like tigecycline which is currently in use [96–98]. Oxytetracycline is the most used tetracycline, with a complicated four-ringed macromolecule with a number of ionisable functional groups. Thus, it is a complex, and zwitterionic organic chemical [99]. In survey by Pham et al. and Chen et al., it was found that the oxytetracycline had a very high risk quotient approximated between 27.78–94.81 g L^{-1} in marine settings [100,101]. Tetracycline's chemical composition is shown in Fig. 9.

It is indeed a concern that the dyes and antibiotics, if left untreated, can contribute significantly to the water pollution. Dyes from the industries such as textile and dyeing, as well as antibiotics from the pharmaceutical manufacturing and health care facilities, can end up in water bodies, leading to the adverse environmental effects. Conventional wastewater dealing approaches, such as physical and chemical processes, may not be sufficient to effectively remove these organic pollutants, therefore, the alternative methods, including photocatalytic degradation are being explored. Photocatalytic degradation is much useful method than the other methods because of its low cost, high degrade efficiency, sustainability and broad applicability.

5. Magnesium ferrite as a photocatalyst

Magnesium ferrite, is a type of spinel ferrite with cubic crystal structure. The magnesium ferrite is represented by the formula, $MgFe_2O_4$ [24,102]. Here Mg is in 2+ state and Fe is in 3+ state. The spinel ferrites are mainly grouped into three categories as per the cationic distribution in their interstitial sites, which are normal, inverse, and mixed. A total of 64 tetrahedral (A-sites) and 32 octahedral sites (B-sites) exists in spinal ferrite unit cell, among these sites 8 A and 16 B-sites are occupied. For typical spinel, divalent cations take up the A-sites while the trivalent cations go to the B-sites. For inverse spinel, trivalent cations occupy the A sites, whereas eight divalent and eight trivalent cations occupy the B-sites. The divalent and the trivalent cations ions are distributed in the tetrahedral (A) site and the octahedral (B) site in case of mixed spinel, respectively. Magnesium ferrite ($MgFe_2O_4$) come under the category of mixed spinel ferrite [103–105]. $MgFe_2O_4$ is the soft type of magnetic substances which have high electrical resistivity and moderate coercivity [106]. It belongs to a type of ternary semiconductor which can effectively absorb the visible light, including a large percentage of the solar spectrum, due to its small bandgap, which is typically in the region of 1.5–3.0 eV. Magnesium ferrite's valence band electrons hops to the conduction band when exposed to light, producing the electron-hole pairs. The mobile charge carriers are then involved in redox interactions with the organic molecules, which leads to their degradation. These traits of $MgFe_2O_4$ ferrite make it suitable for degrading the different types of organic molecules [107]. Due to its high saturation magnetisation, great stability, good magnetic and photocatalytic activity, the Mg ferrite makes a good photocatalyst [24]. The magnetic nature of ferrite enables them to be retracted from the reaction system and be reused several times. This further increases their functionality as they can be sustainably used many times. Although, there are several photocatalysts which are currently being investigated like TiO_2, graphene, g-C_3N_4 and other oxides, and also, have larger band gap, non-magnetic nature, complicated synthesis or low cost-efficiency. That's why, their wide spread use is still debatable. On the other hand, the synthesis and characteristics of the magnesium ferrites have been well established by the various investigators for example, Heidari et al. fabricated the $MgFe_2O_4$ ferrite by utilising the solution combustion method. Different fuels (i.e., citric acid, EDTA, glycine) were utilised for the synthesis of materials. The X-ray diffraction (XRD) results revealed

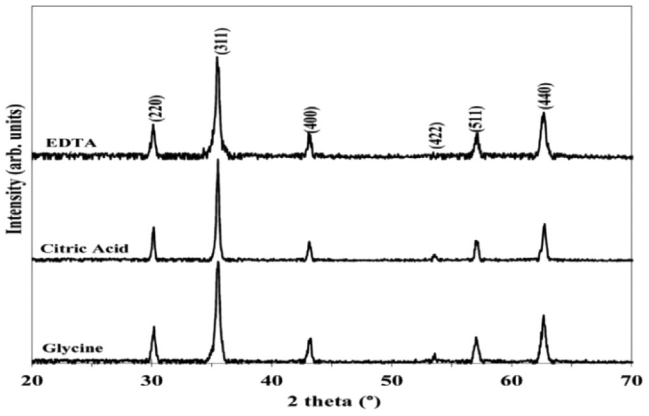

Fig. 10. XRD image of $MgFe_2O_4$ ferrite (reprinted with permission from [108]).

the partially inverse spinel phase of the synthesised samples (Fig. 10).

The crystallite size was found to be dependent on the type of fuel used, and it was highest for the glycine fuel with a size of 57 nm, and the smallest was 35 nm for the EDTA. For citric acid, the crystallite size was 41 nm. Also, the SEM showed the morphologies of different samples (Fig. 11) [108].

Sripriya et al. studied the various traits of $MgFe_2O_4$ synthesised through microwave supported method. Structural analysis through the XRD showed that the lattice parameter obtained was 8.347 Å while the crystallite size was 15.42 nm. The peak positions of XRD correspond to the cubic spinel phase showing the formation of pure phase. Kubelka-Munl model was utilised to analyse the band gap of the synthesised sample and it was 1.91 eV. The synthesised samples were also tested for their photocatalytic behaviour by the degradation of methylene, which was found out to be 96.48%. The higher degradation efficiency was due to the high surface area (71.85 m^2/g) of the samples. This study shows that the even pure magnesium ferrite shows good photocatalytic behaviour for the dye degradation [109]. Singh et al. synthesised $MgFe_2O_4$ by using the sol-gel approach and it was calcinated at 300, 350, 400, and 450°C. Investigations was done to report the affect of calcination temperature on the cation distribution as well as structural and magnetic traits. The production of pure phased $MgFe_2O_4$ was identified by the XRD examination. With calcination, the crystallite size increased. The average cationic distribution between the A- and B-sites was evaluated by XRD data. The cationic distribution demonstrates that the cations move from the B-site to the A-site. M_s increased from 7.52 to 23.54 emu/g as the particle size elevated. The coercivity (H_c) declines with calcination due to a decreasing pinning action at the grain boundary. The curie temperature fell minimal when the A-B exchange contact deteriorated. Fig. 12 shows the hysteresis loops of $MgFe_2O_4$ [110].

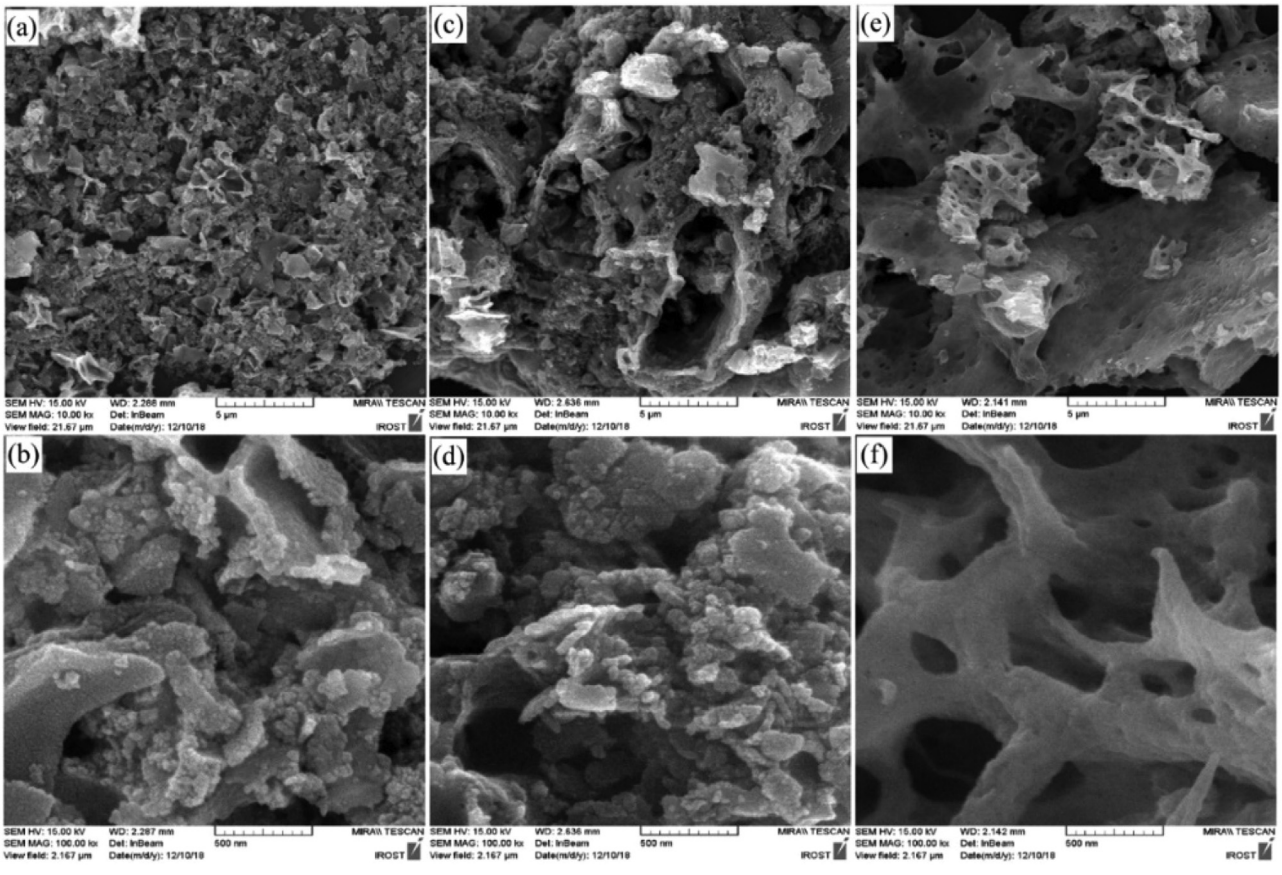

Fig. 11. SEM images of $MgFe_2O_4$ (reprinted with permission from [108]).

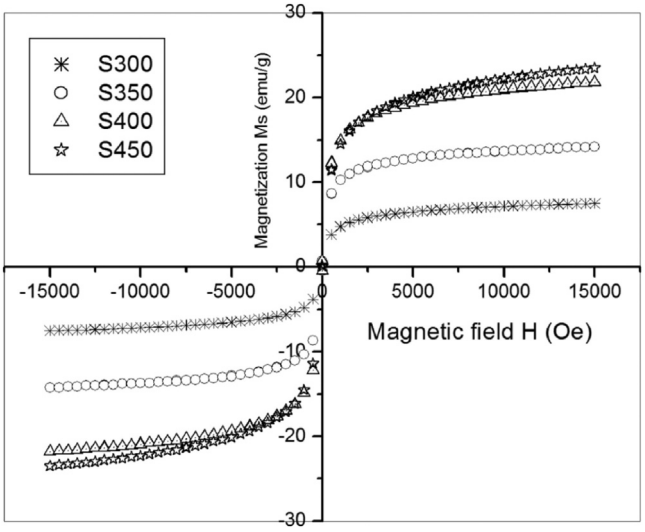

Fig. 12. Hysteresis loop of magnesium ferrite (reprinted with permission from [110]).

All these studies showed that the excellent magnetic and structural qualities of magnesium ferrite underlining their critical importance in permitting the efficient photocatalytic degradation processes. These experiments have also consistently shown that it is feasible to fine-tune the structural and magnetic nature of magnesium ferrite, which opens up a lot of opportunity for improving the general effectiveness of photocatalytic degradation processes. These research studies highlights the positive prospects for utilising the special features of magnesium ferrite in the development of photocatalytic degradation technologies. Table 1 shows the comparative studies of the photodegradation efficiency of magnesium ferrite with the other existing photocatalysts.

5.1. Magnesium ferrite for dye degradation

When used for the dye degradation in wastewater treatment, magnesium ferrite demonstrates the exceptional photocatalytic traits due to its distinct electrical band structure and surface properties. There are many research works which show that the magnesium ferrite can degrade different types of dyes such as non-ionic dyes, cationic dyes and anionic dyes. Nguyen et al. examined the effect of magnesium ferrite on MB decomposition and found that the magnesium ferrite which is calcinated at 500 °C show the degradation of 89.73% and the magnesium ferrite which is calcined at 600 °C show the degradation of 69.17% in 240 min. Magnesium ferrite nanoparticles' surface area and crystal size effect the photocatalytic degradation of MB, as the particles calcinated at 500 °C are smaller in size and have higher degrading efficiency than that of the material calcinated at 600 °C [121]. Fardood et al. researched on the effect of magnesium ferrite for the degradation of MG. The MG was taken in concentration ranging from 5 to 20 mg/l while, the concentration of magnesium ferrite was kept constant at 0.015 g. It was found that the magnesium ferrite can degrade the MG with a percentage of 98% in 60 min [122]. Riyanti et al. inspected the magnesium ferrite for degrading the CR and it was found that the degradation efficiency is 99.62% for CR under the specific conditions. The solution pH was maintained at 6, the Congo red was taken as 10 mg/L and concentration of H_2O_2 was maintained at 2.5 mM with an irradiation time of 180 min [123]. According to the Sundararajan et al., it was found that the magnesium doped cobalt ferrite ($Co_{0.6}Mg_{0.4}Fe_2O_4$) showed the degrading efficiency of 99.5% for the removal of RhB when compared to the pure cobalt ferrite ($CoFe_2O_4$), which has a degrade efficiency of 73.0%. This research shows that the magnesium ferrite has good degrade efficiency for RhB [124]. The study indicated that the magnesium ferrite shows great potential as the efficient photocatalyst for eliminating the different organic dyes.

5.2. Magnesium for antibiotic degradation

Magnesium ferrite demonstrates the remarkable effectiveness not only in the degradation of dyes but also in the efficient breakdown of antibiotics. Organic pollutants like antibiotics are easily degraded by $MgFe_2O_4$ ferrite. There are some studies which show the degradation of antibiotics by the magnesium ferrite. Becker et al. researched about the effect of magnesium ferrite on the degradation of tetracycline and found that at first, magnesium ferrite shows 76% degradation in two hours and after 5 h, 95% degradation was detected [17]. Kadi et al. synthesised $MgFe_2O_4$/g-C_3N_4 using three

Table 1
Comparative studies of the photodegradation efficiency of magnesium ferrite with the other existing photocatalysts.

Composition	Pollutant	Band gap	Degradation efficiency	Reusability	References
$MgFe_2O_4$	Rb21 dye	1.90 eV	93% (180 min)	66% efficiency after 5 cycles	[111]
$MgFe_2O_4/Bi_2WO_6$	Tetracycline hydrochloride	2.23–2.78 eV	95.82% (90 min)	90.18% efficiency after 5 cycles	[112]
$MgFe_2O_4$–CuO/GO	Methylene Blue	1.69 eV	98.8% (27 min)	94.6% efficiency after 4 cycle	[113]
5CQDs/NH_2BDC_{10}-TiO_2	Rhodamine B	2.55–2.60	87.1% (120 min)	–	[114]
TiO_2@TiO_X	Rhodamine B	2.75–3.05	92% (65 min)	–	[115]
TiO_2-FSM-16	Phenol red	–	84% (1220 min)	63% efficiency after 3 cycle	[116]
TiO_2 QDs	Coomassie brilliant blue R dye	3.04–3.18	91% (140 min)	23% decrease after 8 cycle	[117]
ZnO-MoO_3	Rhodamine B	2.25–2.76 eV	94% (120 min)	89% after 5 cycle	[118]
MgO-$CdWO_4$	Bismarck brown	2.4 eV	94% (90 min)	20 to 30% Drop after 5 cycles	[119]
Ce–ZnO–rGO	Bromothymol blue	2.81	92% (180 min)	–	[120]

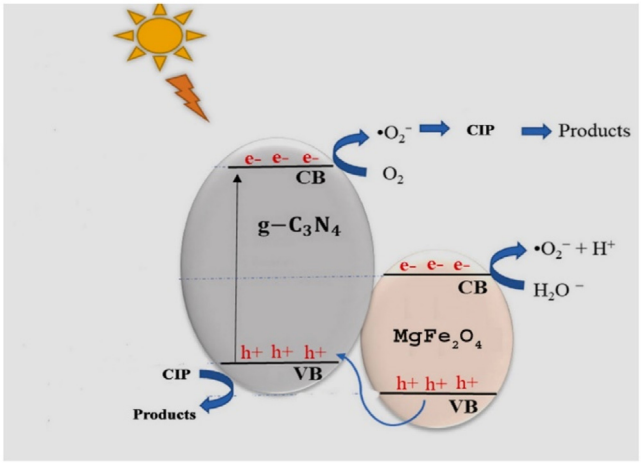

Fig. 13. Schematic of the CIP photodegradation and the charge carriers recombination prevention in the $MgFe_2O_4$/g-C_3N_4 heterostructure (reprinted with permission from [125]).

step synthesis approach. The synthesized composite showed 120 m^2g^{-1} of surface area along with 2.58 eV of band gap. The synthesized samples had a magnetisation of 44.0 emu g^{-1}. The produced samples were utilised in the photocatalytic degradation of ciprofloxacin (CIP). It was found that the composite can degrade the ciprofloxacin almost 100% under the visible light with 1.6 g/L of catalyst. The photocatalysis degradation achieved for the pure g-C_3N_4 and $MgFe_2O_4$ was 10% and 18% correspondingly. The study demonstrated that the hetrostructured composites allowed for the diffusion of CIP in its pores and carried out good charge separation abilities, resulting in enhanced photocatalytic ability (Fig. 13).

The research study also showed that the incorporation of $MgFe_2O_4$ allows for the recyclability of photocatalysts [125]. All these studies shows that the $MgFe_2O_4$ ferrite is a good photocatalyst for the degradation of organic compounds. Magnesium ferrite show more than 90% of the degradation efficiency for many organic compounds. These show that the magnesium ferrite can act as good photocatalyst for the degradation of antibiotics and dyes which make it useful for the water purification. Moreover, the applicability of magnesium ferrite can be extended through the various methods, including doping, synthesis routes, heat treatment, and composite formations.

6. Factors affecting $MgFe_2O_4$ photocatalysis

Photocatalytic degradation of organic compounds by the magnesium ferrite is affected by the different factors such as type of dopant used, synthesis technique, and composites. Some of the factors that are affecting the photocatalytic degradation of magnesium ferrite are discussed below.

6.1. Impact of synthesis

Magnesium ferrite nanoparticles can be formed via synthesis approaches like, co-precipitation, sol-gel combustion, sol-gel, solvent thermal, glycine-nitrate, hydrothermal, ball-milling, etc. [26,126,127]. These synthesis techniques influences the structural and magnetic aspects of the magnesium ferrites thus, creating an overall impact on the degradation efficiency in various ways. The synthesis approaches also have a huge impact on the cost efficiency of magnesium ferrite photocatalysts. The synthesis methods and their impact on the catalytic nature of magnesium ferrite are discussed ahead in detail.

6.1.1. Sol-gel

This is a bottom up approach for the fabrication of nanomaterials. This approach comprise of three parts, first one is making of solution using the appropriate reagent, second one consists of making of the gel using the prepared sol and the third is drying/ageing of gel to get the final product. This reaction was first found through hydrolysis and condensation of metal alkoxides, but this method can also be used for the formation of different metal oxide (binary, ternary and quaternary) using the aqueous metal species. For the preparation of metal semiconductors like ferrites, the most commonly used precursors are metal nitrates (easily soluble and highly oxidising) and citric acid (chelating agent), that's why this method is sometimes also called as the citrate precursor method. The solution of precursors are made in aqueous solvent and some times, the pH regulators like ammonia is also mixed for adjusting the pH. The gel is made through the pyrolysis of solution and sometimes gel precursor like ethylene glycol is also used to fasten up the reaction. After gel formation, the metal nitrates helps during drying due to their strong oxidising nature while the citric acid act as organic fuel and helps in the combustion. This process results in the formation of metal oxides with smaller crystallite size and higher degree of homogeneity, while requiring lesser temperature than the other approaches like solid-state. The gel also ensures the better dissolution of metal ions within the structure and causes the pure phase formation. That's why, many researchers utilise this approach for the formation of ternary and quaternary metal oxides like ferrites. Nguyen et al. examined the impact of synthesis techniques on the crystalline size and degradation efficiency and therefore, it was found that the magnesium ferrite prepared by the combustion method shows the growth in crystalline size from 18 to 61 nm at different calcination. Where the approx particle size was 30 nm and the degrade efficiency of magnesium ferrite for the MB was 89.73% in the presence of light and H_2O_2 [121]. While Cabrera et al. synthesize magnesium ferrite by auto-combustion method and polymerisation method and it was found that the crystallite size was in between 7 and 16 nm where the degrade efficiency of magnesium ferrite for MB was 75% in light [128]. Fardood et al. prepared the magnesium ferrite nanomaterials by the sol-gel method without any organic chemical for the degradation of MG. The crystalline size of magnesium ferrite was 11 nm and it was observed that under the visible light, 98% of the dye was degraded in 60 min. The tests were conducted at 20 mg/L of dye for 60 min of irradiation [122].

6.1.2. Solid state approach

This approach is the most common approach for the preparation of ceramic materials in large scale. This method consists of chemical decomposition of solid reagents at high temperature to form new composition with a well defined structure. This method could be utilised for making the single crystal, thin film, ceramics, polycrystalline material and many more. This method is useful in preparing the metal nitrates, oxides, alkoxides, hydroxides etc. Most commonly used starting precursors are metal oxides. The metal oxides helps in the formation of stable solid solution. This approach requires the high temperature due to the lower activity of solids at lower temperatures. This approach can also be followed at the higher scale by making use of ball mill to perform the mixing. This is also one of the inexpensive approach for the fabrication of nanomaterials. However, as compared to the wet chemical methods like sol-gel, the resulted material from this approach shows the higher degree of agglomeration and bigger particle size with lower homogeneity. Due to the solid-state's accessible and inexpensive nature, researchers are trying to make the efficient photocatalyst from this approach to lower their cost and make them more production friendly. Das et al. fabricated the magnesium ferrite by the facile solid-state reaction technique. The average crystalline size of magnesium ferrite particles was 12.40 nm. It was found that the degrade efficiency of magnesium ferrite for MG was 100% in 50 s in the presence of hydrogen peroxide [129].

6.1.3. Co-precipitation

This is a type of wet chemical approach that consists of separation of solid precipitates from a solution. The starting precursors utilised for this approach consists of acetates, chlorides and nitrates. The solution of metal ions are either made in water or in other organic solvents like ethanol. This process utilies the strong basis in order to start the precipitation of metal cations. The precipitates obtained are washed and dried according to the requirements and they are less agglomerated. The computed crystallite size is smaller as compared to the other approaches. This approach provide the benefits of faster reaction, precise control and the smaller crystallite size, but it needs the use of stronger basis which might become hard to dispose if produced in larger quantities. George et al. adopted the co-precipitation route for the fabrication of Cu doped $MgFe_2O_4$ nanoferrites. The nitrates of metals (Mg, Cu and Fe) were first dissolved in water individually and stirred well. The solutions were mixed together and 2 M NaOH was also mixed to maintain the pH of 13. The resultant mixture was then heated for three hour at 80 °C. The precipitates thus formed were washed and further annealed for 24 h using an oven. The resulted powder was calcinated at 650 °C for 8 h in a furnace. The samples had crystallite size ranging from 12 to 44 nm which was evident from the XRD analysis. The photocatalytic study was done using the UV–Visible spectrum. The samples showed the absorbance in visible range of spectra. To check the photocatalytic behaviour of the samples, MB dye was used. 100 mg of catalyst along with 2 ml of H_2O_2 was utilised to degrade 100 ml of 25 ppm of MB solution. The study was conducted under the UV-lamp for 3 h while the samples were extracted after 30 min. The samples showed a degradation efficiency of 97% towards the MB [130]. Ajeesha et al. fabricated the $Mg_{1-x}Ni_xFe_2O_4$ ($x = 0.0–1.0$) ferrites by co-precipitation route. The nitrates of respective metals were taken as precursor and deionised water was taken as solvent to make a solution. 2 M hydroxides was mixed for maintaining a pH of 13. Then, the heating of mixture for 3 h at 80 °C was done. This resulted in brown coloured precipitates which were separated out by using a centrifuge. The samples were cleaned using distilled water to remove the remaining sodium hydroxides and annealed for 1 day at 75 °C. The powder was subjected to calcination at 650 °C for a period of 8 h using a muffle furnace. The structural study showed that the crystallite size was 24 nm and thus, the cubic phase was attained for all the samples. The samples also showed the higher surface area ranging from 11.757 to 20.478 m^2/g. The photocatalytic investigations were carried out by MB degradation in the visible spectrum. The experiment was performed by utilising the 100 mg of catalysts in 100 ml of MB kept at 25 ppm. 2 ml of H_2O_2 was also used as a sacrificial agent. A 86% of degradation was attained after 3 h of degradation [106].

6.1.4. Hydrothermal

It is a type of heterogeneous wet chemical synthesis for the fabrication of nanomaterials in the aqueous solvent. This synthesis utilises the high pressure to start the crystallisation of desired material. To achieve the desired pressure, auto-clave is utilised. Auto-clave consists of stainless steel body to withstand the pressure and also, the inner part of autoclave is linned with a non reactive material like teflon. Usually water soluble metallic salts like nitrates are used as the precursors for this approach. During the process, the autoclave is heated by making use of furnace and therefore, attains the high pressure which causes the rapid nucleation and causes the formation of fine crystallites. Most of the time, the material obtained from this approach don't need to be calcinated. This process provides the benefits of direct synthesis of material without any need of heat treatment while also being able to maintain the crystallinity of the material. But in hydrothermal method, precautions should be made regarding the applied temperatures to the auto-clave, so that the pressure attained doesn't exceed the limit of the autoclave. Khaliq et al. used the hydrothermal approach for fabricating the pure magnesium ferrite and Ni and Cr doped magnesium ferrite to test its photocatalytic activity against the crystal violet. An autoclave having teflon lining was used for this approach. Firstly, measured amounts of metal nitrates were mixed in deionised water and 25 ml of 1.5 M NaOH was also mixed. The mixture was continuously stirred in the presence of heat which resulted in brown coloured solution. This solution was then passed to the autoclave and heated to 150 °C for a period of 20 h. This resulted in the formation of brownish coloured specimens having pH range between 10 and 11. The specimens were washed using the deionised water to neutralise the pH and also, remove any other contaminates. Finally, the

specimens were dried at 120 °C for four hours to get the final product. The photocatalytic behaviours were measured using the crystal violet dye and the highest degradation efficiency of 97% was achieved within the 100 min of degradation [131].

These studies demonstrated that the synthesis approaches can greatly influence the efficiency of the magnesium ferrite as a photocatalyst. Thus, choosing the appropriate synthesis technique can be helpful for the fabrication of cost-effective and highly efficient magnesium ferrite photocatalyst. Furthermore, the choice of synthesis methods can exert a significant influence on the mass production of magnesium ferrite at an industrial scale. Some synthesis approaches like solid-state approach can be used in industrial scale and can produce the magnesium ferrite in large scale. However, it's worth noting that these physical approaches may compromise the crystallinity of the final product and limit control over the crystallite size. Conversely, the chemical synthesis methods offer greater efficiency in fine-tuning the properties of magnesium ferrite, ensuring the superior control over its characteristics. But, these methods have challenges in terms of scalability, hindering their widespread industrial usages [132–134]. That's why, more research should be done in the synthesis approaches for producing the magnesium ferrite in industrial scale so that it can be more cost-efficient and be used in larger scales.

6.2. Effect of dopant

The photocatalysis by ferrites can be greatly influenced by the doping. Ferrites are a class of materials that are often used in photocatalysis due to their semiconducting properties. There are many ways in which the doping can affect the photocatalytic behaviour of ferrites such as improved stability, reduced band gap, improved charge separation, and reduced crystallite size. It's crucial to keep in mind that the precise impacts of doping on the photocatalytic behaviour of ferrites will depend on the type and number of dopants utilised, as well as the synthesis techniques. Band structure, charge carrier dynamics, and surface chemistry are just a few of the variables that the researchers generally considered when conducting the comprehensive studies to optimise the doping techniques for the photocatalytic applications. Many studies have also shown that the doping has substantial effect on the degradation efficiency of magnesium ferrite. Some of the studies are discussed ahead. Bessy et al. synthesised the cobalt doped magnesium ferrite via the combustion approach. The sample was prepared by mixing 40 ml of egg whites into 60 ml of deionised water followed by the stirring until the homogeneous solution of egg white was obtained. Then, the stoichiometric amounts of metal nitrates were mixed into the egg white mixture and stirred for 60 min until the solution was well dissolved. After that, the mixture was evaporated at 80 °C so that the dried precursor was obtained. Calcination was done at 500 °C for 2 h and the cobalt doped magnesium ferrite was obtained. With the increase in doping of cobalt ferrite, the crystalline size reaches from 23 to 18 nm and also, the degrade efficiency reaches from 91% to 95% [135]. Vishnu et al. prepared $Ni_xMg_{1-x}Fe_2O_4$ (x = 0- 0.6) ferrites through the microwave assisted combustion approach for the removal of rhodamine B and MB. 10 ml of distilled water was combined with the magnesium, nickel, and ferric nitrates for around 30 min. The mixture was then dried in a microwave oven for 30 min. The components were then calcinated for 5 h in a muffle furnace at 600 °C. The components were then characterised and utilised in applications. At 0–120 min time intervals, the $Ni0.4Mg_{0.6}Fe_2O_4$ demonstrated the maximum degradation activity, with MB dye degrading at a rate of 98.1% and RB dye degrading at a rate of 97.9% [136]. Singh et al. prepared $Mg_{1-x}Ti_xFe_2O_{4+\delta}$ (x = 0–1.0) nanoparticles by sol-gel approach for degrading the RhB. It was found that when the doping levels increased, the value of average particle diameter was decreased. $Mg_{0.75}Ti_{0.25}Fe_2O_{4.2}$, $Mg_{0.5}Ti_{0.5}Fe_2O_{4.5}$, and $Mg_{0.25}Ti_{0.75}Fe_2O_{4.75}$ shows the decrease in average particle size by 37.6, 30.7 and 23.4 nm, respectively. It was observed that when the doping of Ti increased from x = 0.0 to 0.5, the band gap showed a steady decrease from 2.53 to 2.24 eV, and also, the band gap improved steadily from 2.24 to 2.44 eV as the dopant concentration increased from 0.5 to 1.0. They performed the photocatalytic degradation using the samples having x = 0.5 under the various pH concentrations because the light absorption rises as the band gap narrows and the lowest band gap was achieved for x = 0.5. Maximum degradation was found to occur at pH 6.0, when it was estimated to be 98% [137]. This study concluded that the doping can greatly alter the degradation efficiencies of magnesium ferrite. It has also been observed that the dopants which reduces the crystallite size can be helpful for increasing the degradation efficiencies.

6.3. Effect of composites

A common method to increase the photocatalyst's photocatalytic degradation efficiency is to create the composite materials. In composites, two or more substances often a photocatalyst and also, another substance are combined to provide the synergistic effects that enhance the overall performance. There are many works that shows, the effect of composition on the photocatalytic degradation of magnesium ferrite. Some of the studies are discussed here. Das et al. prepared the zinc/hydroxyapatite/magnesium ferrite ($Zn/HAP/MgFe_2O_4$) composite for the degradation of MG. Firstly, they synthesised the magnesium ferrite by solid-state reaction, and after that, the composite was made. It was demonstrated that the samples showed 100% degradation efficiency in the presence of H_2O_2. It was also found that the degradation obeyed the first order kinetics [138]. Alhashmi-alameer et al. synthesised the copper doped magnesium ferrite (CMgF), (MgF), and (CMgF@rGo) for the degradation of Benzimidazole and MB. The results shows that the prepared MgF, CMgF and CMgF@rGO samples show the degradation efficiency of 54.54%, 76.5%, 92.4%, respectively for the MB in 240 min. CMgF@rGO shows the degrade efficiency of 50% for Benzimidazole in just 240 min [139]. Kiani et al. prepared

the magnesium ferrite and magnesium titanate composite for the degradation of acid black dye. A 20 ml of ethylene glycol solution was taken in which 0.2 g of PVA was dissolved. Then, 0.1 g of synthetic $MgFe_2O_4$ was mixed in 20 ml of methanol, after that the mixture was subjected to a 15-minute ultrasonic bath. After the 10 min of stirring using magnetic stirrer, 0.22 g of titanium tetra isopropoxide was introduced to the solution (yield of MgTiO3: 0.1 g). Then, 0.5 ml of acetic acid was then introduced, and for 10 min, the mixture was placed in an ultrasonic bath. It took 17 ml of ethylene glycol solution to gradually raise the pH of the mixture in the range of 4 to 5. After that, it was agitated for 2 h in the ultrasonic bath. The resulting mixture spent over the three days in a water bath at 35 °C. After that, the product was dried in an oven for 6 h at 120 °C before being calcinated for 2 h at 700 °C. When compared to the magnesium titanate, which has a degrade efficiency less than 60% in 180 min, the magnesium ferrite and titanate composites have a maximum degradation efficiency of 80% in 180 min [140]. Israr et al. synthesised $(MFO)_{1-x}(GNPs)_x$ composite through the in-situ co-precipitation approach for the degradation of MB. It was observed that under the visible light irradiation, the $(MFO)_{1-x}(GNPs)_x$ composite having $x = 0.25$ showed the photocatalytic activity, degrading 99.3% of MB in 60 min [141].

All of these research studies concluded that the magnesium ferrite photocatalytic efficacies can be influenced by various factors including the synthesis, doping and composite formation, and therefore, a detailed literature study on the impact of these factors on photocatalytic degradation efficiency has been studied in Table 2.

7. Future perspectives and challenges

Although the magnesium ferrite has shown its potential in being a cost-effective and efficient photocatalyst which could be fabricated via a variety of synthesis approaches, there has not been enough research going on in order to increase its photocatalytic abilities.

It is essential to recognise the current constraints impeding the widespread implementation of photocatalytic degradation. Cost-effectiveness, catalyst recovery, and the creation of reliable reactor designs are some of these restrictions. The effective application of magnesium ferrite based photocatalysis in real world wastewater treatment settings depends on addressing these practical issues. It was observed in our study that the doping might be a critical factor in increasing the efficiency of $MgFe_2O_4$ ferrite based photocatalyst, while the other factors like pH, contaminants and the catalysts concentrations also have an impact on the degradation efficiency. Most of the research being done in field of magnesium ferrites showed it efficiency in degrading the organic pollutants under the ideal conditions. Most of the current research being done doesn't account for the real world waste water having multiple types of pollutants. When accounted for the factors like, multiple pollutants, lower visibility, extreme pH and salinity of waste water, there might be larger variation in the degradation

Table 2
Factors affecting the photocatalytic degradation efficiency of $MgFe_2O_4$ ferrite.

Composition	Synthesis	Pollutants	Irradiation	Reaction condition			Degradation		References
				pH	Dose		%	Time (min)	
					Catalyst	Pollutant			
$Mg_{0.8-x}Co_xFe_2O_4$ (x = 0.2- 0.6)	Combustion	Methyl Orange	UV	–	–	-	81	120	[135]
		Methylene Blue					95	120	
$MgFe_2O_4$	Auto-combustion	Methylene Blue	Dark and Visible light	–	–	-	75	35	[128]
$Mg_{1-x}Ti_xFe_2O_{4+\delta}$ (x = 0–1.0)	Sol-gel	Rhodamine B	Visible	6.0	0.01 g/ 100 ml	0.5 ppm	98	120	[137]
$Mg_{0.4}Zn_{(0.6-x)}Ca_xFe_2O_4$	Citrate precursor	Rhodamine B	UV		5 mg/ 100ml	5 g/l	99.5	80	[142]
Cu–$MgFe_2O_4$	Co-precipitation	Methylene Blue	UV		100 mg/100ml	25 ppm	97	180	[130]
$Mn_{0.5}Zn_{0.5-x}Mg_xFe_2O_4$	Sol-gel method	Rhodamine B	UV	11	10 mg/50ml	20 mg/L	95	80	[143]
$Mg_{0.8-x}Zn_xFe_2O_4$, x = 0.2- 0.6	Combustion process	Methylene Blue	UV	–	–	–	92	100	[144]
$Zn_{0.67}Mg_{0.33}Dy_xFe_{2-x}O_4$ (x = 0- 0.02)	Sol-gel auto-combustion	Malachite Green	Visible light	7	0.03 g	15 mg/L	94.23	60	[145]
$MgNd_{0.5x}Dy_{0.5x}Fe_{2-x}O_4$ (x = 0- 0.03)	Sol-gel auto-combustion	Malachite Green	Natural sunlight	7	0.05 g	10 mg/L^-	95.17	60	[102]
$Mg_{1-x}Cu_xFe_2O_4$ (x = 0- 0.5)	Microwave combustion	Tetracycline Hydrochloride	Visible light	6	0.31 g/l	20 mg/l	98.7	165	[146]
$Co_{0.5}Zn_{0.5}Mg_xFe_{2-x}O_4$, x = 0.25–1.0	Citrate precursor	Methylene Blue	Visible light	–	5 mg/100ml	10 mg/L	99.26	60	[147]
$MgFe_2O_4$-Fe_2O_3	Precipitation	Methylene Blue	Solar light	–	0.1 g/100mL	10 mg/L	99.89	120	[148]
$Ni_xMg_{0.5}Zn_{0.5-x}Fe_2O_4$ [x = 0- 0.5]	Co-precipitation	Xylenol Orange	Visible light	-	1 g/L	10 mg/L	90.18	120	[149]
$MgFe_2O_4$/MIL-88A	Ball-milling	Sulfamethoxazole	Visible light	5.8	0.4 g/L	5.0 mg L^{-1}	100	40	[150]
$MgFe_2O_4$@TiO_2	Hydrothermal	Methyl Orange	UV light	–	–	0.5 mM	90	180	[151]

efficiency of pollutants using the magnesium photocatalysts. A detailed analysis on the magnesium ferrite photocatalysis while also accounting for factors like recoverability, reusability, environmental impact, would prove to be useful for further development in this area. Researchers should also focus their attention on the real world implementation of the photocatalysis while also choosing the right method to make it more cost-efficient. The future of magnesium ferrite photocatalysts shows high potential for the waste water treatment but the limitations regarding the real world implementation should be addressed, that way we can fully utilise their potential of being good photocatalysts.

8. Conclusion

Magnesium ferrite, a versatile substance shows potential for treating the water contaminated with organic waste. This review paper emphasises the significant function of magnesium ferrite in this context and highlights the significant value of this material in photocatalytic degradation of dyes and antibiotics. With an excellent average degradation effectiveness reaching 90% in a very short duration of 1–2 h, a number of research investigations have repeatedly shown the significance of magnesium ferrite in degrading a variety of organic pollutants, including azo, dispersion, vat, reactive, and antibiotics. Magnesium ferrite has the potential to be used in the photocatalytic degradation; however, its effectiveness must first be thoroughly examined. Degradation performance can be improved by adjusting the catalyst concentration, pH levels, temperature, and properties of the light source. This review paper promotes future innovations and research in the research field of magnesium ferrite based photocatalysis. This could entail investigating the innovative catalyst modifications and determining whether it is feasible to power the photocatalytic processes using the renewable energy sources. The report also highlights the economic and environmental advantages of using magnesium ferrite for the wastewater treatment. Magnesium ferrite emerges as a catalyst for improvement in the field of green engineering and pollution management by the lowering pollutants, preserving the water resources, and minimising the environmental impact of numerous businesses. Overall, this review paper emphasises the crucial function of magnesium ferrite based photocatalysis of wastewater. While showing its outstanding degrading efficiency, the report also recognises the variables influencing its performance and discusses the practical difficulties that need to be resolved for the widespread deployment. This paper promotes the magnesium ferrite as a useful asset in the pursuit of sustainable and effective wastewater treatment practises by urging the additional study and acknowledging its economic and environmental advantages.

Declaration of competing interest

All authors declare that there are no competing interests.

CRediT authorship contribution statement

Rohit Jasrotia: Writing – review & editing, Writing – original draft, Supervision, Conceptualization, Project administration, Resources. **Nikhil Jaswal:** Writing – original draft. **Jyoti Prakash:** Writing – original draft. **Chan Choon Kit:** Funding acquisition. **Jagpreet Singh:** Writing – review & editing. **Abhishek Kandwal:** Writing – review & editing.

References

[1] M. Shabbir (Ed.), Textiles and Clothing Wiley, 2019, doi:10.1002/9781119526599.
[2] J. Sharma, S. Sharma, V. Soni, Reg. Stud. Mar. Sci. 45 (2021) 101802, doi:10.1016/j.rsma.2021.101802.
[3] K. Ranganathan, S. Jeyapaul, D.C. Sharma, Environ. Monit. Assess. 134 (2007) 363–372, doi:10.1007/s10661-007-9628-z.
[4] J.M. Gozálvez-Zafrilla, D. Sanz-Escribano, J. Lora-García, M.L. Hidalgo, Desalination 222 (2008) 272–279.
[5] M.H. Vijaykumar, P.A. Vaishampayan, Y.S. Shouche, T.B. Karegoudar, Enzyme Microb. Technol. 40 (2007) 204–211.
[6] S. Samsami, M. Mohamadizaniani, M.-H. Sarrafzadeh, E.R. Rene, M. Firoozbahr, Process Saf. Environ. Protect. 143 (2020) 138–163.
[7] Z.U. Zango, A.M. Binzowaimil, O.A. Aldaghri, M.H. Eisa, A. Garba, N.M. Ahmed, et al., Chemosphere 343 (2023) 140223.
[8] K.-T. Chung, J. Environ. Sci Health, Part C 34 (2016) 233–261, doi:10.1080/10590501.2016.1236602.
[9] O.A. Yildirim, M. Bahadir, E. Pehlivan, Feb-Fresenius Environ. Bull. (2022) 33–41.
[10] N. Roy, Alex SA, N. Chandrasekaran, A. Mukherjee, K. Kannabiran, J. Environ. Chem. Eng. 9 (2021) 104796.
[11] F.-T. Tao, C. Hu, J.C. Wu, V.-H. Nguyen, K.-L. Tung, Sep. Purif. Technol. 326 (2023) 124784.
[12] H.Q. Anh, T.P.Q. Le, N. Da Le, X.X. Lu, T.T. Duong, J. Garnier, et al., Sci. Total Environ. 764 (2021) 142865.
[13] R.D. Ambashta, M. Sillanpää, J. Hazard. Mater. 180 (2010) 38–49.
[14] R. Jasrotia, A. Verma, R. Verma, J. Ahmed, S.K. Godara, G. Kumar, et al., J. Water. Process. Eng. 48 (2022) 102865.
[15] R. Kumar, A. Sudhaik, P. Raizada, V.-H. Nguyen, Q. Van Le, T. Ahamad, et al., Chemosphere 337 (2023) 139267.
[16] A. Kumar, P. Singh, V.-H. Nguyen, Q. Van Le, T. Ahamad, S. Thakur, et al., Chem. Eng. J. 474 (2023) 145720.
[17] A. Becker, K. Kirchberg, R. Marschall, Zeitschrift Für Physikalische Chemie 234 (2020) 645–654, doi:10.1515/zpch-2019-1430.
[18] M. Umar, H.A. Aziz, Risk Treat. 8 (2013) 196–197.
[19] R.V. Bharathi, M.K. Raju, P.S.V. Shanmukhi, M.G. Kiran, N. Murali, D. Parajuli, et al., Inorg. Chem. Commun. 158 (2023) 111713.
[20] M. Madhu, A.V. Rao, N. Murali, D. Parajuli, T.W. Mammo, J. Mater. Sci.: Mater. Electron. 34 (2023) 2158, doi:10.1007/s10854-023-11551-y.
[21] T. Tatarchuk, B. Al-Najar, M. Bououdina, M.A. Ahmed, in: Handbook of Ecomaterials, 3, 2019, pp. 1701–1750.
[22] S. Verma, P.A. Joy, Y.B. Khollam, H.S. Potdar, S.B. Deshpande, Mater. Lett. 58 (2004) 1092–1095.
[23] Y. Zu, Y. Zhao, K. Xu, Y. Tong, F. Zhao, Ceram. Int. 42 (2016) 18844–18850.
[24] X. Tian, X. Zhu, Russ. J. Phys. Chem. 95 (2021) 2163–2170, doi:10.1134/S0036024421100290.
[25] F. Naaz, H.K. Dubey, C. Kumari, P. Lahiri, SN. Appl. Sci. 2 (2020) 808, doi:10.1007/s42452-020-2611-9.
[26] R. Kant, A. Mann, A Review of Doped Magnesium Ferrite Nanoparticles: Introduction, Synthesis Techniques and Applications, 2018.
[27] A. Sonune, R. Ghate, Desalination 167 (2004) 55–63.
[28] H. Bill, Pollut. Equipment News (2010) 13.
[29] A.L. Srivastav, M. Ranjan, in: Inorganic Water pollutants. Inorganic Pollutants in Water, Elsevier, 2020, pp. 1–15.

[30] M. Ismail, K. Akhtar, M.I. Khan, T. Kamal, M.A. Khan, A. M Asiri, et al., Curr. Pharm. Des. 25 (2019) 3645–3663.
[31] I.T. Carvalho, L. Santos, Environ. Int. 94 (2016) 736–757.
[32] UNESCO W.UN World Water Development Report, The Untapped Resource, Wastewater, 2017.
[33] G. Crini, E. Lichtfouse, Environ. Chem. Lett. 17 (2019) 145–155.
[34] V. Dutta, A. Sudhaik, R. Kumar, P. Raizada, T. Ahamad, S.M. Alshehri, et al., J. Taiwan. Inst. Chem. Eng. 156 (2024) 105319.
[35] S. Patial, S. Thakur, Q. Van Le, T. Ahamad, P. Singh, V.-H. Nguyen, et al., J. Taiwan. Inst. Chem. Eng. 153 (2023) 105189.
[36] D.B. Miklos, C. Remy, M. Jekel, K.G. Linden, J.E. Drewes, U. Hübner, Water. Res. 139 (2018) 118–131.
[37] E. Fosso-Kankeu, S. Pandey, S.S. Ray, Photocatalysts in Advanced Oxidation Processes For Wastewater Treatment, John Wiley & Sons, 2020.
[38] M. Saeed, M. Muneer, A.U. Haq, N. Akram, Environ. Sci. Pollut. Res. 29 (2022) 293–311, doi:10.1007/s11356-021-16389-7.
[39] A. Kumar, G. Pandey, Mater. Sci. Eng. Int. J. 1 (2017) 1–10.
[40] M. Pavel, C. Anastasescu, R.-N. State, A. Vasile, F. Papa, I. Balint, Catalysts 13 (2023) 380.
[41] A. Fujishima, K. Honda, Nature 238 (1972) 37–38.
[42] U.I. Gaya, A.H. Abdullah, J. Photochem. Photobiol. C: Photochem. Rev. 9 (2008) 1–12.
[43] A. Mills, S Le Hunte, J. Photochem. Photobiol. A: Chemistry 108 (1997) 1–35.
[44] C. Xu, P.R. Anusuyadevi, C. Aymonier, R. Luque, S. Marre, Chem. Soc. Rev. 48 (2019) 3868–3902.
[45] A. Sharma, P.R. Makgwane, E. Lichtfouse, N. Kumar, A.H. Bandegharaei, M. Tahir, Environ. Sci. Pollut. Res. 30 (2023) 64932–64948, doi:10.1007/s11356-023-27093-z.
[46] R. Kumar, P. Raizada, N. Verma, A. Hosseini-Bandegharaei, V.K. Thakur, Q. Van Le, et al., J. Clean. Prod. 297 (2021) 126617.
[47] K. Sharma, V. Dutta, S. Sharma, P. Raizada, A. Hosseini-Bandegharaei, P. Thakur, et al., J. Ind. Eng. Chem. 78 (2019) 1–20.
[48] B.M. Rajbongshi, in: Handbook of Smart Photocatalytic Materials, Elsevier, 2020, pp. 127–149.
[49] M. Han, S. Zhu, S. Lu, Y. Song, T. Feng, S. Tao, et al., Nano Today 19 (2018) 201–218.
[50] W.S. Koe, J.W. Lee, W.C. Chong, Y.L. Pang, L.C. Sim, Environ. Sci. Pollut. Res. 27 (2020) 2522–2565, doi:10.1007/s11356-019-07193-5.
[51] A. Ajmal, I. Majeed, R.N. Malik, H. Idriss, M.A. Nadeem, RSC. Adv. 4 (2014) 37003–37026.
[52] A. Rani, K. Singh, A.S. Patel, P. Sharma, Bull. Mater. Sci. 46 (2023) 94, doi:10.1007/s12034-023-02929-z.
[53] Pereira L., Alves M. In: Malik A, Grohmann E, editors. Environmental Protection Strategies For Sustainable Development, Dordrecht: Springer Netherlands; 2012, p. 111–62. https://doi.org/10.1007/978-94-007-1591-2_4.
[54] R.L.M. Allen, in: Colour Chemistry, Springer US, Boston, MA, 1971, pp. 103–137, doi:10.1007/978-1-4615-6663-2_8.
[55] O.A. Attallah, M.A. Al-Ghobashy, M. Nebsen, M.Y. Salem, RSC. Adv. 6 (2016) 11461–11480.
[56] Benkhaya S., M'rabet S., Lgaz H., El Bachiri A., El Harfi A. In: Muthu SS, Khadir A, editors. Dye Biodegradation, Mechanisms and Techniques, Singapore: Springer Singapore; 2022, p. 1–50. https://doi.org/10.1007/978-981-16-5932-4_1.
[57] W.A. Al-Amrani, M.A.K.M. Hanafiah, A.-H.A Mohammed, Environ. Sci. Pollut. Res. 29 (2022) 76565–76610, doi:10.1007/s11356-022-23062-0.
[58] E. Rápó, S. Tonk, Molecules 26 (2021) 5419.
[59] R. Jasrotia, J. Prakash, G. Kumar, R. Verma, S. Kumari, S. Kumar, et al., Chemosphere 294 (2022) 133706.
[60] A.A. Al-Gheethi, Q.M. Azhar, P.S. Kumar, A.A. Yusuf, A.K. Al-Buriahi, R.M.S.R. Mohamed, et al., Chemosphere 287 (2022) 132080.
[61] P. Zhou, Z. Dai, T. Lu, X. Ru, M.A. Ofori, W. Yang, et al., Catalysts. 12 (2022) 669.
[62] T.L. Yusuf, B.O. Orimolade, D. Masekela, B. Mamba, N. Mabuba, RSC. Adv. 12 (2022) 26176–26191.
[63] A. Thakur, H. Kaur, Int. J. Ind. Chem. 8 (2017) 175–186, doi:10.1007/s40090-017-0113-4.
[64] Z.M. Şenol, N.E. Messaoudi, Y. Fernine, Z.S. Keskin, Biomass Conv. Bioref. (2023), doi:10.1007/s13399-023-03781-1.
[65] N. Nasseh, F.S. Arghavan, S. Rodriguez-Couto, A. Hossein Panahi, Int. J. Environ. Anal. Chem. 102 (2022) 2342–2362, doi:10.1080/03067319.2020.1754810.
[66] M. Harja, G. Buema, D. Bucur, Sci. Rep. 12 (2022) 6087.
[67] M.B. Mobarak, N.S. Pinky, F. Chowdhury, M.S. Hossain, M. Mahmud, M.S. Quddus, et al., J. Saudi Chem. Soc. 27 (2023) 101690.
[68] M. Hernández-Zamora, F Martínez-Jerónimo, Environ. Sci. Pollut. Res. 26 (2019) 11743–11755, doi:10.1007/s11356-019-04589-1.
[69] R.R.M. Khan, H. Qamar, A. Hameed, A.U. Rehman, M. Pervaiz, Z. Saeed, et al., Water. Air. Soil. Pollut. 233 (2022) 468, doi:10.1007/s11270-022-05935-9.
[70] M.I. Din, R. Khalid, J. Najeeb, Z. Hussain, J. Clean. Prod. 298 (2021) 126567.
[71] V. Soni, A. Sudhaik, P. Singh, S. Thakur, T. Ahamad, V.-H. Nguyen, et al., Chemosphere 347 (2024) 140694.
[72] P. Kotwal, R. Jasrotia, J. Prakash, J. Ahmed, A. Verma, R. Verma, et al., Environ. Res. (2023) 116103.
[73] S.P. Raghuvanshi, R. Singh, C.P. Kaushik, A. Raghav, Appl. Ecol. Environ. Res. 2 (2004) 35–43.
[74] H.B. Slama, A. Chenari Bouket, Z. Pourhassan, F.N. Alenezi, A. Silini, H. Cherif-Silini, et al., Appl. Sci. 11 (2021) 6255.
[75] F. Mashkoor, A. Nasar, J. Magn. Magn. Mater. 500 (2020) 166408.
[76] S. Srivastava, R. Sinha, D. Roy, Aquat. Toxicol. 66 (2004) 319–329.
[77] M. Getaye, S. Hagos, Y. Alemu, Z. Tamene, O.P. Yadav, J. Anal. Pharm. Res. 6 (2017) 00184.
[78] G.L. Hoffman, F.P. Meyer, Parasites of freshwater fishes. A review of their control and treatment. Parasites of Freshwater Fishes A Review of Their Control and Treatment, 1974.
[79] D.J. Alderman, J. Fish. Dis. 8 (1985) 289–298, doi:10.1111/j.1365-2761.1985.tb00945.x.
[80] S.J. Culp, F.A. Beland, J. Am. Coll. Toxicol. 15 (1996) 219–238, doi:10.3109/10915819609008715.
[81] C. Fernandes, V.S. Lalitha, K.V.K. Rao, Carcinogenesis 12 (1991) 839–845.
[82] K.V.K. Rao, Toxicol. Lett. 81 (1995) 107–113.
[83] J.L. Martinez, Environ. Pollut. 157 (2009) 2893–2902.
[84] R. Gothwal, T. Shashidhar, CLEAN Soil Air Water 43 (2015) 479–489, doi:10.1002/clen.201300989.
[85] O.M.D SAÚDE (OMS), Overcoming Antibiotic Resistance. World Health Organization Report in Infectious Diseases, 2000.
[86] M. Beiranvand, S. Farhadi, A. Mohammadi-Gholami, RSC. Adv. 12 (2022) 34438–34453.
[87] S. Shehu Imam, R. Adnan, N.H Mohd Kaus, Toxicol. Environ. Chem. 100 (2018) 518–539, doi:10.1080/02772248.2018.1545128.
[88] M.A. Parra, N.E. Cerquera, C.P. Ortiz, R.E. Cárdenas-Torres, D.R. Delgado, M.Á. Peña, et al., J. Taiwan. Inst. Chem. Eng. 150 (2023) 105028.
[89] J.V. Kumar, R. Karthik, S.-M. Chen, V. Muthuraj, C. Karuppiah, Sci. Rep. 6 (2016) 34149.
[90] M. Seifrtová, A. Pena, C.M. Lino, P. Solich, Anal. Bioanal. Chem. 391 (2008) 799–805, doi:10.1007/s00216-008-2020-1.
[91] D.J. Larsson, C. de Pedro, N. Paxeus, J. Hazard. Mater. 148 (2007) 751–755.
[92] N.G. Vengerovich, V.V. Perelygin, Pharm. Formulas 3 (2021) 66–71.
[93] N. Martins, R. Pereira, N. Abrantes, J. Pereira, F. Gonçalves, C.R. Marques, Ecotoxicology 21 (2012) 1167–1176, doi:10.1007/s10646-012-0871-x.
[94] P. Sun, S. Zhou, Y. Yang, S. Liu, Q. Cao, Y. Wang, et al., Adv. Compos. Hybrid. Mater. 5 (2022) 3158–3175, doi:10.1007/s42114-022-00462-x.
[95] M. Jia, Q. Liu, W. Xiong, Z. Yang, C. Zhang, D. Wang, et al., Appl. Catal. B: Environmental 310 (2022) 121344.
[96] M. Orylska-Ratynska, W. Placek, A. Owczarczyk-Saczonek, Int. J. Environ. Res. Public Health 19 (2022) 7246.

[97] L.B. Pickens, Y. Tang, J. Biol. Chem. 285 (2010) 27509–27515.
[98] A. Rusu, E.L. Buta, Pharmaceutics. 13 (2021) 2085.
[99] Z. LI, W. QI, F. Yao, Y. LIU, S. Ebrahim, L Jian, J. Integr. Agric. 18 (2019) 1953–1960.
[100] Y. Chen, X. Xi, G. Yu, Q. Cao, B. Wang, F. Vince, et al., Front. Environ. Sci. Eng. 9 (2015) 394–401, doi:10.1007/s11783-014-0653-1.
[101] D-G Kim, S.-O. Ko, Chemosphere 191 (2018) 639–650.
[102] G. Katoch, J. Prakash, R. Jasrotia, A. Verma, R. Verma, S. Kumari, et al., J. Water. Process. Eng. 53 (2023) 103726.
[103] M. Amiri, K. Eskandari, M. Salavati-Niasari, Adv. Colloid. Interface Sci. 271 (2019) 101982, doi:10.1016/j.cis.2019.07.003.
[104] A. Soufi, H. Hajjaoui, R. Elmoubarki, M. Abdennouri, S. Qourzal, N Barka, Appl. Surf. Sci. Adv. 6 (2021) 100145.
[105] D.H.K. Reddy, Y.-S. Yun, Coord. Chem. Rev. 315 (2016) 90–111.
[106] T. Ajeesha, A. Ashwini, M. George, A. Manikandan, J.A. Mary, Y. Slimani, et al., Physica B: Condens. Matter 606 (2021) 412660.
[107] M. Easwari, S. Jesurani, Int. Res. J. Eng. Technol. 4 (2017) 110–113.
[108] P. Heidari, S.M. Masoudpanah, J. Mater. Res. Technol. 9 (2020) 4469–4475.
[109] R.C. Sripriya, M. Mahendiran, J. Madahavan, M.V.A. Raj, Mater. Today: Proceedings 8 (2019) 310–314.
[110] R.P. Singh, C. Venkataraju, Chin. J. Phys. 56 (2018) 2218–2225, doi:10.1016/j.cjph.2018.07.005.
[111] R. Jarariya, K. Suresh, Mater. Today: Proceedings 72 (2023) 2618–2629.
[112] H. Zhang, F. Meng, H. Wei, W. Yu, S. Yao, J. Colloid. Interface Sci. 652 (2023) 1282–1296.
[113] I.F. Waheed, O.Y.T. Al-Janabi, P.J. Foot, J. Mol. Liq. 357 (2022) 119084.
[114] J. Shi, C. Ju, T. Yang, J. Shi, K. Pu, T. Zhao, et al., Colloids Surf. A: Physicochem. Eng. Aspects 677 (2023) 132378.
[115] J. Zeng, Y. Huang, Int. J. Hydrogen Energy 51 (2024) 423–432.
[116] S.M. Mousavi, S.H. Meraji, A.M. Sanati, B. Ramavandi, Heliyon. 9 (2023).
[117] W.A. Mohamed, H.H. Abd El-Gawad, H.T. Handal, H.R. Galal, H.A. Mousa, B.A. ElSayed, et al., Opt. Mater. 137 (2023) 113607.
[118] M.K. Hussain, N.R. Khalid, M. Tanveer, A. Abbas, F. Ali, W. Hassan, et al., Opt. Mater. 148 (2024) 114794.
[119] A.H. Jawhari, M.A. Malik, N. Hassan, B. Fatima, J. Mol. Struct. (2024) 137594, doi:10.1016/j.molstruc.2024.137594.
[120] M. Haruna, F. Eshun, C.K. Bandoh, E.S. Agorku, O. Francis, N.K. Asare–Donkor, et al., Sustain. Chem. Environ. (2024) 100069.
[121] L.T. Nguyen, L.T. Nguyen, N.C. Manh, D.N. Quoc, H.N. Quang, H.T. Nguyen, et al., J. Chem. 2019 (2019) 1–8.
[122] S. Taghavi Fardood, F. Moradnia, M. Mostafaei, Z. Afshari, V. Faramarzi, S Ganjkhanlu, Nanochem. Res. 4 (2019) 86–93.
[123] F. Riyanti, N. Nurhidayah, W. Purwaningrum, N. Yuliasari, P.L. Hariani, Environ. Nat. Resour. J. 21 (2023) 322–332.
[124] M. Sundararajan, L. John Kennedy, P. Nithya, J. Judith Vijaya, M Bououdina, J. Phys. Chem. Solids 108 (2017) 61–75, doi:10.1016/j.jpcs.2017.04.002.
[125] M.W. Kadi, R.M. Mohamed, D.W. Bahnemann, Opt. Mater. 121 (2021) 111598.
[126] R. Sagayaraj, Int. Nano Lett. (2022), doi:10.1007/s40089-022-00368-y.
[127] I. Chihi, M. Baazaoui, N. Hamdaoui, J.M. Greneche, M. Oumezzine, Farah Kh, J. Mater. Sci.: Mater. Electron. 32 (2021) 16634–16647, doi:10.1007/s10854-021-06218-5.
[128] A.F. Cabrera, C.R. Torres, S.G. Marchetti, S.J. Stewart, J. Environ. Chem. Eng. 8 (2020) 104274.
[129] K.C. Das, S.S. Dhar, J. Alloys. Compd. 828 (2020) 154462.
[130] M. George, T.L. Ajeesha, A. Manikandan, A. Anantharaman, R.S. Jansi, E.R. Kumar, et al., J. Phys. Chem. Solids 153 (2021) 110010.
[131] N. Khaliq, I. Bibi, F. Majid, M.I. Arshad, A. Ghafoor, Z. Nazeer, et al., Results Phys. 43 (2022) 106059.
[132] P.G. Jamkhande, N.W. Ghule, A.H. Bamer, M.G. Kalaskar, J. Drug Deliv. Sci. Technol. 53 (2019) 101174.
[133] K. Pal, S. Chakroborty, N. Nath, Green Process. Synth. 11 (2022) 951–964, doi:10.1515/gps-2022-0081.
[134] E.M. Modan, A.G PLĂIAŞU, Metall. Mater. Sci. 43 (2020) 53–60.
[135] T.C. Bessy, M.R. Bindhu, J. Johnson, R. Rajagopal, P. Kuppusamy, Chemosphere 299 (2022) 134396.
[136] G. Vishnu, S. Singh, N. Kaul, P.C. Ramamurthy, T. Naik, R. Viswanath, et al., Environ. Res. 235 (2023) 116598.
[137] G. Singh, M. Kaur, V. Kumar Garg, A.C Oliveira, Ceram. Int. (2022), doi:10.1016/j.ceramint.2022.05.067.
[138] Das KCh, S.S. Dhar, J. Mater. Sci. 55 (2020) 4592–4606, doi:10.1007/s10853-019-04294-x.
[139] D. Alhashmialameer, S. Ullah, A. Irshad, I.A. Alsafari, H.H. Abd El-Gawad, M.A. Abdelrahman Elsheikh, et al., Ceram. Int. 48 (2022) 24100–24113, doi:10.1016/j.ceramint.2022.05.373.
[140] A. Kiani, G. Nabiyouni, S. Masoumi, D. Ghanbari, Compos. Part B: Engineering 175 (2019) 107080.
[141] M. Israr, J. Iqbal, A. Arshad, P. Gómez-Romero, R. Benages, Solid. State Sci. 110 (2020) 106363, doi:10.1016/j.solidstatesciences.2020.106363.
[142] S. Kumari, N. Dhanda, A. Thakur, V. Gupta, S. Singh, R. Kumar, et al., Ceram. Int. (2022).
[143] M.A. Maksoud, G.S. El-Sayyad, A.M. El-Khawaga, M. Abd Elkodous, A. Abokhadra, M.A. Elsayed, et al., J. Hazard. Mater. 399 (2020) 123000.
[144] T.C. Bessy, M.R. Bindhu, J. Johnson, S.-M. Chen, T.-W. Chen, K.S. Almaary, Environ. Res. 204 (2022) 111917, doi:10.1016/j.envres.2021.111917.
[145] R. Jasrotia, A. Verma, R. Verma, S.K. Godara, J. Ahmed, A. Mehtab, et al., Ceram. Int. (2022).
[146] L. Rajadurai, C.S. Dash, S. Revathi, A.T. Dhiwahar, M. Sundararajan, et al., Inorg. Chem. Commun. 162 (2024) 112197.
[147] D. Chahar, D. Kumar, P. Thakur, A. Thakur, Mater. Res. Bull. 162 (2023) 112205.
[148] J.P. Dhal, S.K. Sahoo, B.G. Mishra, G. Hota, Mater. Lett. 196 (2017) 95–99.
[149] A.V. Bagade, S.N. Pund, P.A. Nagwade, B. Kumar, S.U. Deshmukh, A.B. Kanagare, Catal. Commun. (2023) 106719.
[150] K.-X. Shi, F. Qiu, P. Wang, H. Li, C.-C. Wang, Sep. Purif. Technol. 301 (2022) 121965.
[151] R.P. Ummer, P. Gopinath, N. Kalarikkal, S. Thomas, in: AIP Conference Proceedings, 2082, AIP Publishing, 2019.